Available online at www.sciencedirect.com

SciVerse ScienceDirect

Physics Procedia 37 (2012) 1537 – 1545

Physics Procedia

TIPP 2011 – Technology and Instrumentation for Particle Physics 2011

Study of Highly Pixelated CdZnTe Detector for PET Applications

Yongzhi Yin[a,b,*], Ximeng Chen[a], Sergey Komarov[b], Heyu Wu[b], Jie Wen[b], Henric Krawczynski[c], Ling-Jian Meng[d], Yuan-Chuan Tai[b]

[a]*School of Nuclear Scinence and Technology, Lanzhou University, Lanzhou 730000, China*
[b]*Deparment of Radiology, Washington University in St.Louis, MO 63110, USA*
[c]*Department of Physics, Washington University in St.Louis, MO 63110, USA*
[d]*Department of Nuclear, Plasma and Radiological Engineering, University of Illinois at Urbana-Champaign, IL 61822, USA*

Abstract

We are investigating the feasibility of a high-resolution PET insert device based on a Cadmium Zinc Telluride (CdZnTe) detector with 350μm anode pixel pitch to be integrated into a conventional animal PET scanner to improve its image resolution to sub-500 micrometer range. In this work, we have used a simplified version of the future 2048-pixel CdZnTe planar detector with 250μm anode pixel size and 100 μm gap. This simplified 9 anode pixel structure makes it possible to conduct experiments without a complete ASIC readout system (with 2048 channels) that is still under development. We characterized this CdZnTe detector by investigating it charge sharing, spatial resolution, and energy resolution. We imaged a Na-22 point source using the coincidence events between this 350μm pixelated CdZnTe detector and a lutetium oxyorthosilicate (LSO) based Siemens Inveon PET detector. The reconstructed PET image shows a resolution of 590 μm full width at half maximum (FWHM) by using single-pixel events. When we included double-pixel charge sharing events in the image reconstruction, the image resolution was degraded to 655μm, but the sensitivity of the coincidence system increased 2.5 to 3 times.

Keywords: CdZnTe detector; Charge sharing; Spatial resolution; PET imaging;

* *Emaill*: yinyzh@lzu.edu.cn

1875-3892 © 2012 Published by Elsevier B.V. Selection and/or peer review under responsibility of the organizing committee for TIPP 11. Open access under CC BY-NC-ND license. doi:10.1016/j.phpro.2012.04.105

1. Introduction

Positron emission tomography (PET) has been widely used in both clinical diagnosis and animal research. The image resolution of PET is mainly limited by three factors: positron range, acolinearity effect, and intrinsic spatial resolution of detector. Tai *et al.* proposed Virtual-Pinhole PET geometry to improve the image resolution of PET [1, 2], which uses a high-resolution detector insert device in coincidence with general-purpose whole-body or animal PET scanners. Similar research of this geometry can also be found in Zoom-in PET [3, 4]. Sub-millimeter PET image resolution was obtained by using an insert device (LSO based) integrated into a microPET F-220 system (Siemens Molecular Imaging, Inc.) [5]. These encouraging results prompted us to continue searching for high-resolution detector technologies to further extend the image resolution of animal PET scanners.

The use of a CdZnTe detector as a PET detector has been investigated by several groups. In general, the spatial resolution of a pixelated CdZnTe detector is limited by the anode pixel size. However, the spatial resolution of such a detector is also limited by the charge sharing between the neighboring anode pixels that collect the electrons created after gamma-ray interaction. For the calculation of charge sharing, the original electron cloud size and the diffusion of the electrons should be taken into account. Electron cloud size is dependent on the energy deposited, and the diffusion of the electron is dependent on the detector biased voltage and the thickness of the detector. Charge sharing decreases the detection efficiency of single-pixel photopeak events and increases the fraction of multiple-pixel photopeak events. While pixelated CdZnTe detectors have been widely studied and characterized over the last decades [6], limited work has been done at the 350μm pitch level for PET imaging applications.

In this work, we investigate the feasibility of a pixelated CdZnTe detector as a high-resolution gamma detector for imaging applications, with a particular emphasis in PET insert applications. We characterize the charge sharing property of a prototype simplified pixelated CdZnTe detector and its intrinsic spatial resolution. We also measured the image resolution of a VP-PET system using the prototype CdZnTe detector in coincidence with a Siemens Inveon PET detector. Based on this preliminary study, we outline future work needed in order to fully realize the potential of pixelated CdZnTe detector for PET insert applications.

2. Experimental materials and methods

One of the major challenges in using pixelated CdZnTe detectors is to read out accurately and efficiently thousands (or more) of channels of anode signals. An application specific integrated circuit (ASIC) is currently being developed at the University of Illinois at Urbana-Champaign for semiconductor gamma-ray detectors based on CdTe or CdZnTe. This ASIC has 2048 channels of preamplifiers and analog-to-digital converters (ADC) with 350μm pixel pitch. Since this ASIC is not yet available, we used in this study a 9 anode pixels (3-by-3) CdZnTe detector. A 20 mm × 20 mm × 5 mm CdZnTe substrate from former Orbotech Medical Solutions was polished and contacted with coplanar cathode and 350 μm pixels anode structure in a class-100 clean room in our institution [7, 8]. The anode mask of custom designed 9-pixel pattern is shown in Fig.1.A. The pixel pattern has a central 250 μm pixel and 8 surrounding 250μm pixels. The gap between pixels is 100 μm. The 8 neighbor pixels are connected with eight 1.4mm circle pads 2.5 mm away. The area surrounding the anodes and circle pads is connected to ground to provide the same potential for the anode pixels and the rest of the anode surface. It is expected that the central anode of the 9-anode detector will be representative of the regular 350μm pitch pixelated CdZnTe detectors that we plan to use in the future.

2.1. Charge sharing

In this experiment, we investigate the charge sharing of 350μm pixelated CdZnTe detector and measure the energy resolution for double-pixel events – events that involve two CdZnTe anode pixels. Charge sharing between the central pixel and its neighboring pixels was measured using non-collimated sources, Co-57 and Na-22. The CdZnTe detector was mounted in a holder made of milled Ultem plastic using gold-plated, spring-loaded electric probes (pogo-pins) to connect the anode pixels with readout traces on a printed circuits board (PCB). The 9 anode signals and the coplanar cathode signal were connected to 10 channels of preamplifiers (AMPTEK A250) as shown in Fig.2.A. The pre-amplified CdZnTe signals were fed into a 16 channels spectroscopy amplifier (CAEN N568) using a shaping time of 3 μs. The shaped CdZnTe detector signals were acquired by two 12-bit 600 kHz ADC cards (PCI-417 by Datel) in a PC using the unshaped fast signal from the anode A5 (the center pixel) of the prototype CdZnTe detector as the trigger. The amplitude of the single-pixel event is based on the integration of charge detected by A5, while the amplitude of the double-pixel event is a sum of the signals from A5 and A4 (the neighboring pixel to the left of A5).

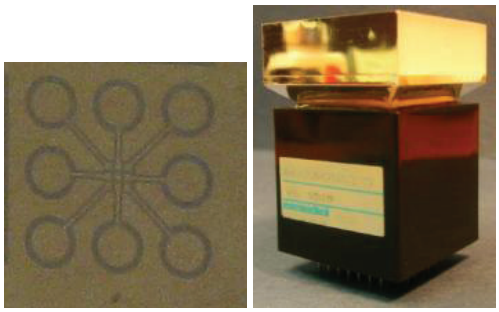

Fig. 1 (A) 9-pixel pattern of custom design CdZnTe detector; (B) Siemens Inveon PET detector module with LSO crystals.

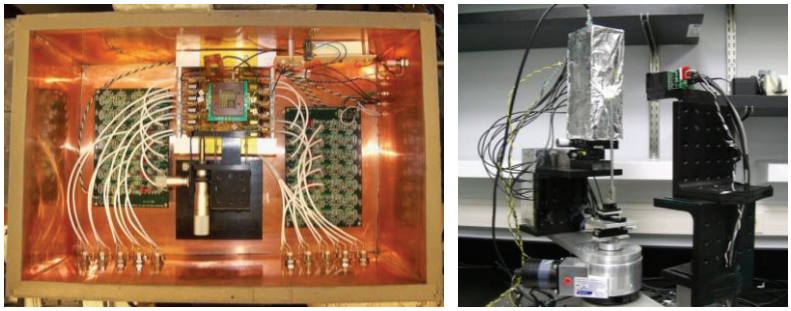

Fig. 2 (A) A copper shielding box with AmpTek A250 preamplifiers; (B) Experimental setup for coincidence measurement between the CdZnTe and LSO detectors.

2.2. Spatial resolution.

For a VP-PET insert system, the intrinsic spatial resolution of a high-resolution gamma-ray detector (CdZnTe detector in this case) is the dominant component of the achievable spatial resolution. In this experiment, the intrinsic spatial resolution of the 350μm pixelated CdZnTe detector was measured using a collimated gamma-ray source of 122keV and 511keV using the setup in Fig.3. The collimator for 511keV gamma-ray source has much thicker tungsten blocks, as shown in Fig.3.C. And the entrance of the

511keV collimator is much bigger than the slit of 122keV collimator because of the difficulties in machining tungsten alloy with 3.5cm thickness.

To show charge sharing between adjacent anode pixels and to evaluate the intrinsic spatial resolution of 350 μm pitch pixelated CdZnTe detectors, we stepped the collimated Co-57 source across the central anode pixel (A5) and its two neighboring anode pixels (A4 and A6). The collimator was made of two layers of slit collimation with a 25μm slit entrance on top and a 330μm slit in the middle to create an effective collimated gamma- ray beam size of about 80 μm × 625 μm. During the experiments, we moved the collimator along the narrow beam direction in a step size of 50.4 μm. We studied the distribution of charges between anode pixels in different source locations. We analyzed the photopeak events that involved single-pixel detection (charge collected by the central anode pixel only) and double-pixel detection (charge collected by the central pixel and one of the two neighboring anode pixels) in all collimator locations. The measured count distribution profile was expected to be the convolution of the detector intrinsic resolution and collimator beam profile. The FWHM of the measured count distribution profile can be reasonably approximated by the quadratic sum of the FWHM of the two individual components.

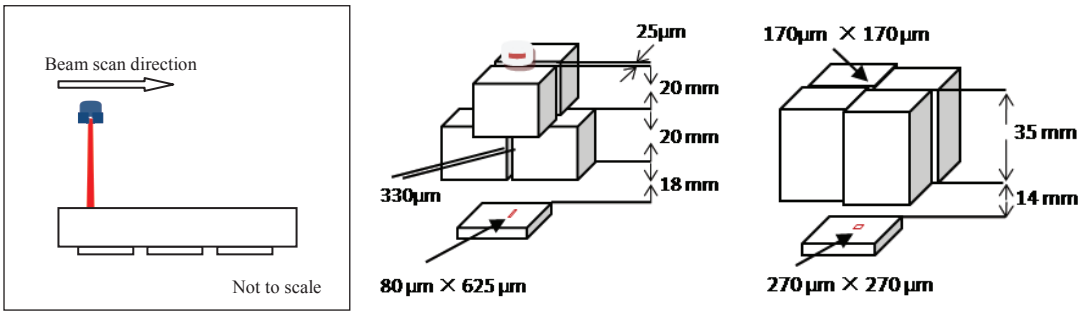

Fig. 3 (A) Illustration of spatial-resolution measurement using a collimated 122keV beam scanned cross three pixels; (B) The collimator of tungsten blocks for Co-57 source; (C) The collimator of tungsten blocks for Na-22 source, ref. [13].

2.3. PET imaging experiment

Virtual-Pinhole PET is based on the coincidence setup with asymmetric detector sizes to create a region with high spatial resolution near the small detector. By inserting a high-resolution detector into a conventional PET scanner, one could get high-resolution PET images within a reduced imaging field of view and still maintain the high-sensitivity of the PET scanner.

Siemens Inveon system is considered the current state-of-art for preclinical imaging research using small laboratory animals. Our goal is to develop a high-resolution PET insert device that can be integrated into an existing animal PET system to provide ultrahigh resolution PET images. So, we chose to use an Inveon PET detector to setup the coincidence measurement with our prototype CdZnTe detector. The Inveon PET detector module consists of a 20 × 20 array of LSO crystals, with 1.59 mm crystal pitch and 1.53×1.53×10 mm crystal size (Fig.1.B), coupled to a position-sensitive photomultiplier tube (Hamamatsu R8900 C12 PSPMT) via a tapered multiple-element light guide. Details in the performance and characterization of the Inveon system can be found in literature [9].

To set up the coincidence detection, the signals of the CdZnTe detectors and the Inveon PET detector were both processed by the same 16-channels spectroscopy amplifier above, but with different shaping time and gain (3μs for CdZnTe and 1μs for LSO). The fast unshaped signals of CdZnTe and LSO detectors from the spectroscopy amplifier were passed through two Fan-In/Fan-Out modules to trigger

two constant fraction discriminators (CFD), which were subsequently fed into a logic unit for coincidence determination. We used two ADCs to digitize the shaped CdZnTe signals and the LSO-PMT signals that have very different timing characteristics from each other. The two ADCs had to be triggered at different times in order to sample CdZnTe and LSO-PMT signals at the correct time points when the shaped waveforms reached their peaks.

In this experiment, we used a 350 μm pitch pixelated CdZnTe detector as the high-resolution insert detector, and used a 1.6mm pitch Inveon LSO detector to mimic the PET scanner with lower resolution detector. The distance between the center of rotation (COR) and the CdZnTe detector is 23mm, and the distance between COR and LSO detector is 127mm. We estimated the reconstructed image resolution near the center of field of view (FOV) of the above geometry is about 585μm FWHM using the equation in [1]. By using one 350 μm CdZnTe pixel in coincidence with a LSO block detector, the FOV of our setup is ~40mm in diameter. We placed a Na-22 source (250 μm in diameter and embedded in an acrylic cube) in the FOV, as shown in Fig.2.B. The source activity was 11 μCi. The coincidence setup consists of two motor-driven concentric rotation stages. By rotating independently the two detectors mounted on the two stages, we were able to record the coincidence events from all possible angles. The coincidence events acquired from different angles were sorted to form a fan-beam sinogram and subsequently reconstructed using a fan-beam filtered back-projection (FBP) algorithm to form PET images [10].

3. Results and discussions

3.1. Charge sharing

As a room temperature gamma-ray detector, CdZnTe detector has shown excellent energy resolution. For 662keV gamma rays, groups have achieved ~1% FWHM energy resolution if the correction of electron loss was properly done [6]. Due to the small pixel effect [11], pixelated CdZnTe detector's energy resolution and spatial resolution have been shown to improve as the pixel size decreases. However, this tendency may not hold true when the pixel size becomes very small relative to the size of charge cloud created by the gamma-ray interacting with the detector. For 350 μm pitch CdZnTe detector, charge sharing events (double and multiple) are dominant, and lead to decrease in the energy resolution of the detector and the detection efficiency of single-pixel events.

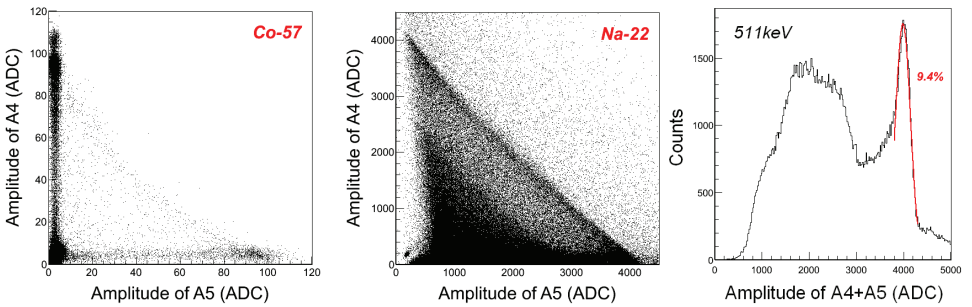

Fig. 4 (A) and (B) show, respectively, the scatter plots of A5 versus A4 for Co-57 and Na-22 source measurements; (C) shows the energy spectrum of double-pixel events of 511keV source measurement, the amplitude is the sum of the two signals A5 and A4.

The characterizations of 350 μm pitch CdZnTe detectors show charge sharing increases with gamma-ray energy. As shown in Fig.4.A and Fig.4.B, the double-pixel charge-sharing events increase with gamma-ray energy, which could be easily understood by the bigger cloud size and more Compton-

scattering events that created by higher-energy photons. In the measurements of Fig.4.A and Fig.4.B, we use respectively non-collimated Co-57 and Na-22 sources. The source position in these two measurements remains the same. In the measurement of 122keV source, we triggered our data acquisition system by either pixels A4 or A5 signals. Given the asymmetric 9-pixel geometry, the pixel A4 that was connected to a big readout pad will receive more events to trigger the data acquisition system. With this observation, we changed the setup to only trigger by the central pixel A5 when we used the 511keV source. Fig4.C shows the energy spectrum of double-pixel events measured using a Na-22 non-collimated source. In this analysis, we summed up the signal amplitudes of two pixels, central pixel A5 and neighbor pixel A4. The energy resolution of double-pixel events is about 9.4% (raw data, no DOI correction) for 511 keV photopeak. The readout-electronics noise contribution is about 0.6%.

3.2. Spatial resolution

Fig.5. shows the detected count profiles of 350μm pixelated CdZnTe detector biased at -800V when a collimated 122keV beam scanned across three pixels in the central row. The square dots are the count profiles of single-pixel photopeak events measured by central pixel A5 when a collimated source was stepped across the anode A5. The circle (or triangle) dots show the count profiles of double-pixel photopeak events measured by the central pixel A5 and its neighboring pixel A4 (or A6) when the collimated source was stepped across the anodes and the gap between them.

For 122keV gamma rays, the profile of single-pixel events detected by A5 shows approximately 250μm FWHM, which is equal to the pixel size. The count rate of single-pixel photopeak events reaches its peak at the center of the pixel A5. The count rate of double-pixel photopeak events reaches its peak at the center of the gaps between adjacent pixels. At the same time, the separation of the peak position of the two double-pixel profiles (circle and triangle dots) is equal to the pixel pitch 350μm. The results suggest that, for 122keV gammas, the intrinsic spatial resolution of a 350μm pitched pixelated CZT detector is approximately equal to the anode pixel size. The ratio of double-pixel events to total events (sum of single pixel events and double-pixel events) is ~ 70%. The charge sharing profile (circle dots) is slightly wider than the previously reported 125 μm FWHM measured at -1000V [12]. This can be explained by (1) a reduced bias voltage (-800V) leads to longer electron drift time and thus more diffusion and charge sharing; (2) charge loss of CdZnTe detector biased at -800V can be more severe than charge loss of the detector biased at -1000V.

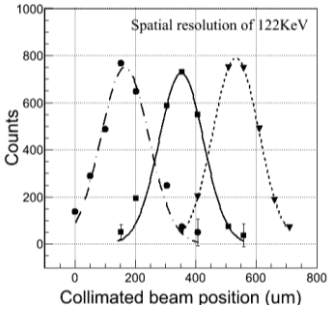

Fig. 5 profile of spatial resolution of 350μm pixelated CdZnTe detector biased at -800V, square dots are single-pixel events detected by A5, circle (triangle) dots are double pixel events detected by A5 and A4 (A6); the smooth curves are Gaussian fit to the data.

The detected count profile of a Na-22 beam was measured with a different collimator, which has much thicker tungsten blocks to attenuate the 511keV gamma rays, as shown in Fig.3.C. Experiments suggest that, for 350 μm pitch pixelated CdZnTe detector, the FWHMs of the count profiles of both single-pixel events and double-pixel events increase with gamma-ray energy, from 122keV to 511keV. This can be explained by the larger charge cloud size and the higher probability of Compton scattering caused by higher energy gamma rays. Details will become available in a paper under review [13].

Monte Carlo simulation was also performed to estimate the position resolution of current 350μm pixelated CdZnTe detector using the same collimator setup. The results of experiment and simulation are in reasonable agreement. The main differences between the experiment and simulation results are in the tails of the count profiles of single-pixel events and double-pixel events. The detailed description of the MC simulation can be found in [14].

3.3. PET Imaging experiment

Fig.6 shows PET images of a Na-22 point source. If we only include single-pixel photopeak events (detected by A5) for image reconstruction, the average image resolution is 670 μm FWHM. This image resolution includes the source dimension (250μm in diameter) and positron range (approximately 200 μm FWHM of blurring effect). If we subtract the effective source dimension, the resolution of the image of the single-pixel photopeak events is estimated to be around 590μm FWHM.

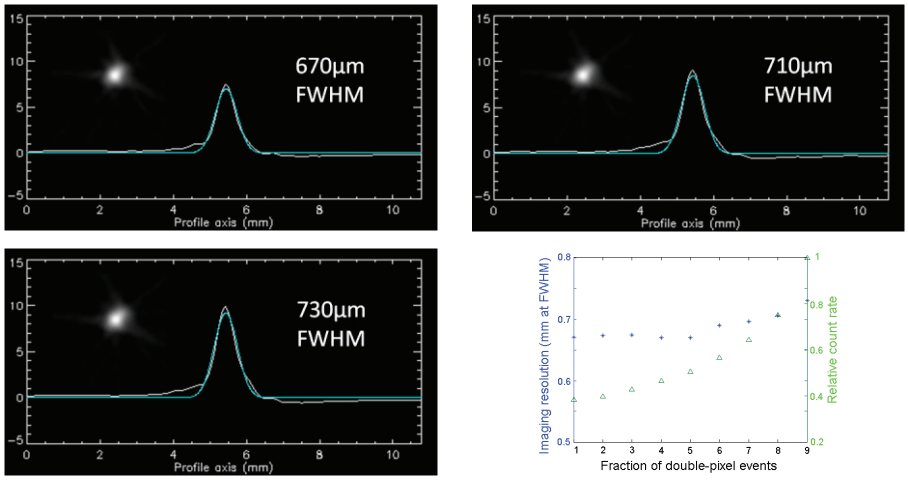

Fig. 6 FBP reconstructed PET images including single-pixel events and different fraction double-pixel charge sharing events; (A. Upper left) image resolution of single-pixel events; (B. Upper right) image resolution of single pixel events and some fraction of double-pixel events; (C. Lower left) image resolution of single pixel events and all double-pixel events; (D. Lower right) the relation of imaging resolution and sensitivity of the system with various fractions of double-pixel events.

To evaluate how the double-pixel charge sharing events affect the image resolution, we included different fractions of double-pixel photopeak events for image reconstruction and re-calculated the image resolution for each. The selection criteria are based on the charge collected by central pixel (A5) and neighbor pixels. First, we only included those events with the central pixel amplitude greater than 9 times the amplitude of neighbor pixels. Those events are very similar to single-pixel photopeak events. Then, we included more double-pixel charge sharing events until the signal amplitude of the central pixel is equal to the signal amplitude of the neighboring pixel. When all double-pixel charge sharing events are

included, but the central anode pixel still has the highest signal amplitude compared with the amplitudes of all 9 pixels, the image resolution decreases to ~ 730 μm FWHM (655μm FWHM if corrected for the source dimension and positron range). However, the sensitivity of the coincidence system increases 2.5 to 3 times. The image resolution and the relative count rate (or sensitivity) of the system were plotted as a function of the included double-pixel photopeak events (indexed by "ratio of A5 signal and A4 signal") and shown in the Fig.6.D.

4. Conclusions

We have characterized the 9-pixel 350 μm pitch pixelated CdZnTe detector, including charge sharing, spatial resolution, and energy resolution. By using this CdZnTe detector in coincidence with a LSO-based Inveon PET detector, we imaged a Na-22 point source (250μm in diameter, embedded in an acrylic cube). The results suggest:

1) For 350 μm pitch pixelated CdZnTe detector, the spatial resolution in 2D is approximately equal to the pixel pitch, 350μm; energy resolution of both single-pixel event and double-pixel events are better than 9%.
2) Using 350 μm pitch pixelated CdZnTe detector, we obtained 670 μm FWHM reconstructed PET image resolution using single-pixel events. When we included double-pixel charge sharing events in the reconstruction (the central anode pixel still has the highest signal amplitude compared with the amplitudes of all 9 pixels), the image resolution decreased to 730 μm FWHM, but the sensitivity of the system improved 2.5 to 3 times. The image resolution of the system is estimated to be 590 and 655 μm FWHM for the single-pixel and double-pixel events, respectively, if the effective source dimension is subtracted.

In conclusion, the use of 350μm pixelated CZT detector as a PET insert in an animal PET scanner shows significantly improved image resolution (600μm to 700μm). However, this value is worse than the imaging resolution we expected (500μm to 600μm) from theoretical calculations. Further investigation is needed to improve the coincidence detection setup. We plan also to improve the analysis and utilization of double-pixel events from the CdZnTe detector, possibly through interpolation of event positioning using charge sharing information. We expect that the image resolution of the system can be further improved once these corrections and interpolations are optimized.

Acknowledgements

This work was supported in part by the U.S. Department of Energy under Grant No. DEFG0208ER64681, and in part by the Chinese Scholarship Council (No. 2008618034). We thank Dr. Joseph A. O'Sullivan and Mr. Paul Dowkontt for their valuable discussions.

References

[1] Tai Y C, Wu H, Pal D, and O'Sullivan J A, "Virtual-pinhole PET," J. Nucl. Med., vol. 49, no. 3, pp. 471-479, 2008.
[2] Chatziioannou A, "VP-PET: A new imaging modality?," J. Nucl. Med., vol. 49, no.3, pp. 345–346, 2008.
[3] Zhou J and Qi J, "Theoretical analysis and simulation study of a high-resolution zoom-in PET system," *Phys. Med. Biol.*, vol. 54, pp. 5193-5208, 2009.
[4] Qi J, Yang Y, Zhou J, Wu Y, Cherry S R, "Experimental Assessment of Resolution Improvement of a Zoom-in PET," *Phys. Med. Biol.*, vol. 56, N165-N174, 2011.
[5] Wu H, Pal D, Song T, O'Sullivan J A, and Tai Y C, "Micro Insert: A prototype full-ring PET device for improving the image resolution of a small-animal PET scanner," J. Nucl. Med., vol. 49, no. 10, pp. 1668-1676, 2008.

[6] Kim J C, Anderson S E, Kaye W, Zhang F, Zhu Y, Kaye S J, and He Z, "Charge sharing in common-grid pixelated CdZnTe detectors, " Nucl. Instr. And Meth. A., vol. 654, pp. 233-243, 2011.
[7] Li Q, Beilicke M, Lee K, Garson III A, Guo Q, Martin J, Yin Y, Dowkontt P, Geronimo G De, Jung I, and Krawczynski H, "Study of thick CZT detectors for X-ray and Gamma-ray astronomy," Astroparticle Physics, vol. 34, no.10, pp. 769-777, 2011.
[8] Jung I, Krawczynski H, Burger A, Guo M, and Groza M, "Detailed studies of pixelated CZT detectors grown with the modified horizontal Bridgman method," Astroparticle Physics, vol. 28, no. 4-5, pp. 397-408, 2007.
[9] Constantinescu C C and Mukherjee J, "Performance evaluation of an Inveon PET preclinical scanner, " Phys. Med. Biol., no. 54, pp. 2885–2899, 2009.
[10] Pal D, O'Sullivan J A, Wu H, Janecek M, and Tai Y C, "2D linear and iterative reconstruction algorithms for a PET-insert scanner,"Phys. Med. Biol., vol. 52, pp. 4293-4310, 2007.
[11] Barrett H H, Eskin J D, and Barber H B, "Charge transport in arrays of semiconductor gamma-ray detectors," Phy. Rev. L, vol. 75, no.1, pp. 156-159, 1995.
[12] Yin Y, Komarov S, Wu H, Song T Y, Li Q, Garson A, Lee K, Simburger G, Dowkontt P, Krawczynski H, and Tai Y C, "Characterization of highly pixelated CdZnTe detectors for sub-millimeter PET imaging," Nucl. Sci. Symp. Conf. Rec., pp. 2411-2414, 2009.
[13] Yin Y, Wu H, Komarov S, Garson A, Guo Q, Krawczynski H, Meng L J and Tai Y C, "3D spatial resolution of 350μm pitch pixelated CdZnTe detector for imaging applications," Submitted to IEEE Trans. Nucl. Sci., 2011.
[14] Komarov S, Yin Y, Wu H, Wen J, Krawczynski H, Meng L J, and Tai Y C, "Study of highly pixelated CdZnTe detector for PET imaging," Submitted to Phys. Med. Biol., 2011.